Crop Leaf Area Index Observations With a Wireless Sensor Network and Its Potential for Validating Remote Sensing Products

Yonghua Qu, Yeqing Zhu, Wenchao Han, Jindi Wang, and Mingguo Ma

***Abstract*—The collection of ground measurements for validating remotely sensed crop leaf area index (LAI) is labor and time intensive. This paper presents an automatic measuring system that was designed based on a wireless sensor network (WSN). The corn LAI was continuously observed from June 25 to August 24, 2012. Approximately, 42 in situ WSN measurement nodes were used in a 4×4 km^2 area in the Heihe watershed of northwest China. The data were analyzed in three ways: 1) a comparison with LAI-2000, 2) a daily and 5-day aggregated time series analysis, and 3) a comparison with a Moderate Resolution Imaging Spectroradiometer (MODIS) LAI using both a ground LAINet LAI and a scaled-up LAI through inversion of Advanced Spaceborne Thermal Emission and Reflection radiometer (ASTER) data. The preliminary results indicated that the measured LAI values from the LAINet were correlated with the values derived from LAI-2000 (R2 from 0.27 to 0.96 with an average of 0.42). When compared with the daily crop LAI growth trajectory, the performance of the measurement system was improved by using the data that were aggregated over a 5-day window. When compared with MODIS LAI, we found that the spatial aggregation values of the ground LAINet observations and the scaled-up ASTER LAI were identical or similar to the MODIS LAI values over time. With its low-cost and low-energy consumption, the proposed WSN observation system is a promising method for collecting ground crop LAI in flexible time and space for validating the remote sensing land products.**

***Index Terms*—Leaf area index (LAI), remote sensing, validation, wireless sensor network (WSN).**

I. Introduction

LEAF area index (LAI) is defined as half of the leaf surface area per horizontal ground area unit and is an important parameter for ecological and hydrological modeling [1]. Estimation of the LAI using remote sensing data has been an important method for obtaining LAI data at regional and global scales. However, the LAI that is estimated from remote sensing data must be validated and evaluated using ground measurements before it can be used as a reliable input parameter for other models [2].

LAI ground validation methods are classified as either direct or indirect [3]. The direct method is considered to be the most reliable for LAI ground truth. However, due to its low efficiency, the direct method can only be used to obtain the ground LAI reference values, which are used to calibrate other indirect measuring instruments.

For this reason, the remote sensing LAI validation experiments rely largely on indirect measurement methods. In the most indirect method, the LAI is measured from multi-angle canopy transmittance under specified conditions [4]. For example, the LAI-2000 (Li–Cor, Lincoln, Nebraska, USA) should be measured in diffuse light. Furthermore, the approximately real-time total downward solar radiation must be measured in open spaces or outside of the canopy. Next, the ratio of the two measurements can be used to calculate the canopy transmittance [5]. Unlike the LAI-2000, which uses diffuse light, DEMON (CSIRO, Canberra, Australia) repeatedly measures direct radiation [6]. The sensor needs to move linearly over a certain distance underneath the canopy during measurement, and the measurements must be repeated several times between early morning and noon to collect the data across a range of zenith angles.

For instruments that do not use an imaging method, the total incidence outside of the canopy and the radiation that permeates through the canopy are measured. Therefore, the successful application of these instruments is determined by their efficiency, ease of use, and accuracy. In practice, the operators must walk outside of the canopy of large croplands or woodlands to find an open area each time the incident solar radiation is measured [7]. This type of measurement greatly reduces the efficiency of these instruments [8]. Therefore, some instruments are designed with cable or radio links. To calculate and display LAI values in real time, sensors inside and outside of the canopy share the data collection terminal. Cables and radio link technology are used to transmit the measured sensor values outside of the canopy to the data collector [4]. However, the cable-based data generation is inconvenient for operators inside of the canopy because they must take measurements while walking. In contrast, radio link transmission is only effective at communication distances of 150–200 m [4]. These limitations create problems when ground validating the remotely sensed parameters.

Although the instrument measurement mode (which relies on an individual walking the interior of the experimental site

Manuscript received April 28, 2013; revised October 05, 2013; accepted October 29, 2013. Date of publication November 21, 2013; date of current version January 30, 2014. This work was supported in part by the National Natural Science Foundation of China (91125004, 41271348), the National Basic Research Program of China (2013CB733403), and in part by the National High Technology Research and Development Program (2012AA12A303).

Y. Qu, Y. Zhu, W. Han, and J. Wang are with the State Key Laboratory of Remote Sensing Science, Beijing Key Laboratory for Remote Sensing of Environment and Digital Cities, School of Geography, Beijing Normal University, Beijing 100875, China (e-mail: qyh@bnu.edu.cn).

M. Ma is with the Laboratory of Remote Sensing and Geospatial Science, Cold and Arid Regions Environmental and Engineering Research Institute Chinese Academy of Sciences, Lanzhou 730000, China (e-mail: mmg@lzb.ac.cn).

Color versions of one or more of the figures in this paper are available online at http://ieeexplore.ieee.org.

Digital Object Identifier 10.1109/JSTARS.2013.2289931

with the measurement devices to obtain multiple sample values) improves the LAI measurement efficiency, this mode is labor intensive and requires long periods of sample collection over large areas. Because the ground measurements are constrained by the satellite revisit time, they are generally completed several days before or after the satellite revisits the experimental site in ground synchronous or quasi-synchronous experiments. To validate the LAI at a resolution of 1 km, e.g., a Moderate Resolution Imaging Spectroradiometer (MODIS) LAI, it is assumed that the ground experiments require ground-based observational data with a range of at least 2×2 MODIS pixels. Therefore, it is difficult to obtain LAI data over such a large space and a short time period.

Due to the difficulty of ground validating the remote sensing data, practical experience suggests that joint remote sensing experiments that are conducted by multiple research entities provide an effective way to carry out ground validation work [9]. In reality, however, multiple research groups use multiple observation instruments at the same time, which produces uncertainty in the LAI ground measurements. For example, each observation instrument applies to a distinct condition because of its particular measurement principle. These differences result in deviations that reach or exceed 50% between different instruments [3], [6], [10]. Therefore, it is difficult to ensure the data quality when different instruments are used at the same time. Furthermore, different operators obtain different measurement results, even when using the same type of instrument. This is caused by uncertainty in the operator's approach. Although human uncertainty can be reduced by developing measurement standards [11], these uncertainties remain an obstacle to obtain the consistent data.

Some researchers have noted the difficulty of using traditional instruments to express LAI variations in space, and continuity in time, from data measured at a single node. It has also been suggested that movable or sufficiently long linear array sensors might solve this problem [4]. Lang *et al.* proposed a collection of multiple measurements at close proximity under the canopy, which would measure the transmittance of inhomogeneous canopies and calculate the canopy LAI [7], [12]. To collect this data, however, drive motors must be deployed or operators must walk under the canopy. Although these principles promote the successful development of commercial LAI measurement systems, they are more applicable to small measurement areas. If the measurement range is large, this method requires massive amount of labor. Ryu *et al.* hoped to obtain the data automatically by observing the data from different measurement instruments and interconnecting them with a wireless network [8]. If implemented in the future, this method may reduce manual operation and allow for continuous observations in space. Other researchers have indicated that a simple and replicable method for obtaining a ground sample of vegetation parameters is important for ecological observations [13], [14] and for the application of remote sensing data [15].

In the field of earth observations, a new method based on wireless sensor network (WSN) technology, which is called the earth observation sensor web (EOSW), has gained an increasing attention [16], [17]. The EOSW has been preliminarily applied in many research fields such as sea ice, soil moisture, and environmental monitoring [16], [18]. Currently, in terms of vegetation WSN monitoring, a significant amount of work has been performed to measure the environmental parameters (such as temperature and moisture) of vegetation growth [14], [19]–[22]. However, few studies have evaluated the automatic measurement system of vegetation LAI. Compared to the newly emerging EOSW technique, over the past 20 years, ground-based LAI measurements have developed relatively slowly. In this context, we have started to consider the possibility of using the existing WSN technology to automatically measure the vegetation LAI. A few pioneering researchers have also started to consider this possibility. Yuan *et al.* reported a WSN prototype system for automatically measuring the canopy LAI [23]. This system deploys an optical sensor under the canopy to capture the vegetation canopy transmittance and calculates the LAI based on the Beer–Lambert law. However, due to the heterogeneity of canopies, the transmittance obtained from a single sensor is not enough to represent the transmittance of the entire canopy. Therefore, it is difficult to represent the heterogeneity of canopy LAI using this method.

Cheaper automatic LAI measurements, which can be used for large areas, are critical for ground validation experiments of remote sensing surface parameters. These systems should be designed to save energy, to make simultaneous observations of a large number of measured points in space, and to ensure continuous observation over time. Based on the direct light transmittance algorithm for measuring the LAI, we developed an LAI measurement system: LAINet [24]. LAINet is a low-cost LAI network measurement system based on WSN technology. This paper aims to validate LAINet performance based on the aspects of multi-node measurements in space and continuous measurements in time.

Overall, this study has the following aims:

1) to develop a WSN system to take automatic LAI measurements that are suitable for validating the remotely sensed products;
2) to validate the performance of the newly developed canopy structure measurement system and conduct a comparative analysis of the commonly used LAI measurement instruments; and
3) to compare the LAI measured from developed WSNs with MODIS products and analyze their time variation characteristics.

II. Methods

A. Experimental Design

The field experiments presented in this paper were a part of the Heihe watershed allied telemetry experimental research (HiWATER) project, which is a multi-disciplinary and integrated remote sensing experiment evaluating ecological and hydrological processes in the Heihe River basin [9]. An artificial oasis in the middle reach of the Heihe River was selected as the experimental area. This area is located in the Yingke and Daman irrigation districts (longitude: $100°40'$E, latitude: $38°80'$N). The observations were made between June and August, 2012. Corn was selected for the study because it is an atypical row crop that is planted uniformly with noncontinuous gaps in experimental area. Plant spacing of 10–20 cm and row spacing of 50–70 cm were used.

TABLE I
COST-EFFICIENCY OF TRADITIONAL INSTRUMENTS VERSUS LAINET[a]

	Hardware cost			Labor (work days)			
	Single price	Number	Total ($)	Deploying cost	Per measurement cycle	Maintain	Total
LAI-2000	$8000	2	$16000	0	4–32	0	32–416
LAINet	$250	90	$22500	6	0	3	9

[a]The cost in this table is approximately estimated.

LAINet is an automatic device that obtains multi-angle transmittance of the vegetation canopy during the day following the sun's movement, based on WSN technology, and then calculates the crop LAI from multi-angle transmittance using a vegetation gap probability model. This WSN consists of three different node types. The first node type is a circle node with three light sensors that are deployed above the canopy to receive the total downward solar radiation. Next, the linear node types are used that have nine light sensors under the canopy and that receive the permeated radiation. Finally, sink nodes are used to collect and transmit the data to a remote data server through the general packet radio service (GPRS) network. Communication between the nodes is implemented with a Zigbee network, which is based on the standard IEEE 802.15.4 low-power field network protocol. Detailed information regarding the system architecture can be found in Qu [24].

If only a few measurements in a small space are needed, LAINet is not as advantageous as traditional LAI measurement instruments. However, if continuous long time-series observations are carried out at a large regional scale, LAINet has the following advantages:

1) It can reduce the time required for one to access the experimental site. LAINet only requires one to enter the experimental site during instrument deployment and, therefore, can minimize the plant disturbances by the experimenter, which is not possible with current traditional instruments.
2) Multiple measurement nodes are automatically synchronized, which ensures that the measured data of each node are obtained simultaneously and avoids the data uncertainty caused by the differences in measurement time.
3) Wireless communication among measurement nodes requires no wiring. Communication both among the nodes under the canopy and among the nodes under and above the canopy is completed via Zigbee wireless networks. As a result, there is no need to lay and connect cables in the open area or under the canopy to facilitate the instrument deployment.
4) The field data are remotely transmitted to the data center via public wireless networks and are automatically saved on the database server. Human labor is not required to collect the field data.
5) It reduces the data acquisition costs, including instrument and labor costs. For example, in a 3×3 km^2 sampling region, following the Validation of Land European Remote Sensing Instruments (VALERI) [25], 30–50 elementary sampling units are required. Traditional measurements take approximately 4–32 days of labor to complete the weekly repeated measurements. For a growth time of 3 months and a sampling frequency of 7 days, e.g., approximately 13 times the observations are required to obtain continuous observed data over such a long period of time. The approximate cost-efficiency comparison between LAINet and traditional instruments (e.g., LAI-2000) is given in Table I.

Table I shows that in a validation experiment, such as the one that was conducted in a 3×3 km^2 area, the difference in the hardware cost between the two types of observation strategies is not obvious. However, as stated previously, there is a distinct advantage of LAINet in terms of labor cost.

In terms of the validation of LAI products, a spatial sampling method is an important component of the product validation specification. In a VALERI project group, researchers have proposed many ground sampling methods [26], [27] to validate the medium- and low-resolution LAI products. The literature summarized the three sampling methods that were commonly used in the current LAI validation. In practice, it is often necessary to adjust the existing sampling methods depending on the specific situation. In our 2012 experimental scheme, the spatial sampling of the LAI adopted an approximately uniform sampling method. Namely, within a range of 4×4 km^2, one to multiple LAINet measurement nodes was deployed in the space corresponding to each MODIS pixel. Theoretically speaking, the surface variability at the MODIS pixel scale should be taken into account. However, due to the limitation of the sensor nodes in our first experiment, the number of ground nodes is not calculated strictly in accordance with the spatial variability in the current work. In fact, we usually deploy a smaller number of nodes under relatively uniform vegetation than under nonuniform vegetation. In the practical deployment of LAINet nodes, the selection of node locations takes two factors into account: first, the best use of existing observational results is considered. Before the deployment of LAINet nodes, multiple soil moisture WSN nodes are deployed in the experimental area [9]. The deployment of soil moisture measurement nodes accounts for the spatial differentiation of soil moisture. Although it is impossible that the spatial variability of LAINet would be fully consistent with that of the moisture, we assume that the spatial variability of the crop LAI is mainly controlled by the soil moisture. Therefore, the nodes that we deployed were basically the same as the existing soil moisture nodes. Secondly, easy instrument installation is involved. To minimize the disturbance to the crop caused by instrument installation, we utilized the existing experimental infrastructure. For example, the below-canopy nodes were designed to share

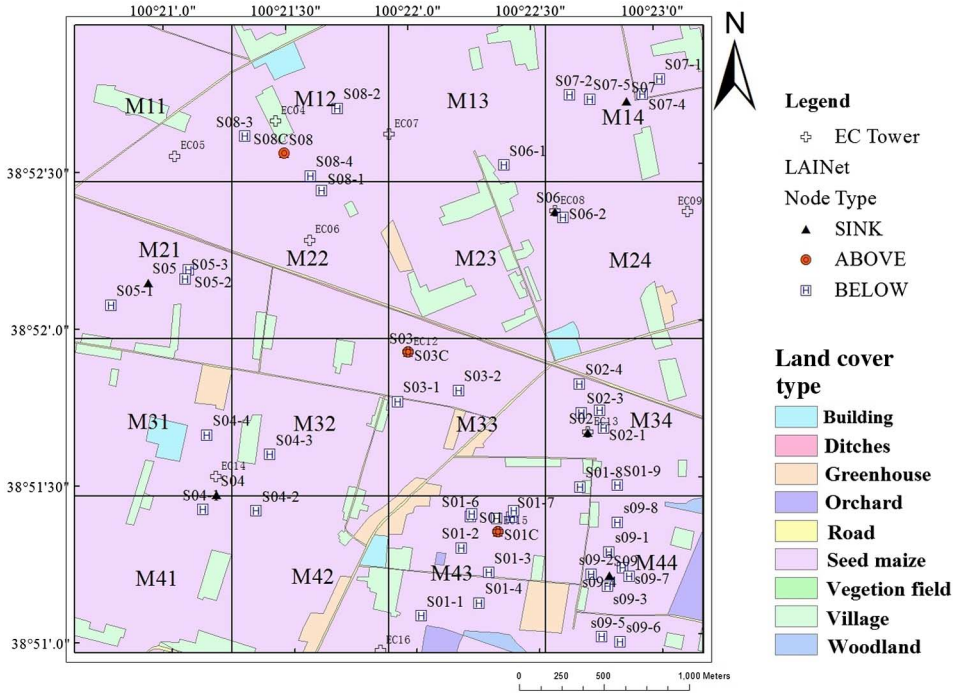

Fig. 1. Instrument nodes deployment map in the experimental area. There are 9 sink nodes (S01–S09) and 42 measurement nodes under the canopy ($S0_{i-j}$: i stands for the sink node number and j stands for the measurement node number below the sink nodes), 3 measurement nodes for total radiation above the canopy (S01C, S02C, and S03C), and 15 eddy covariance matrix towers (EC01–EC15) with 4×4 MODIS pixels ($M_{ij},\ i,\ j = 1, 2, 3, 4$).

antenna brackets with soil moisture nodes, and some sink nodes were arranged to share the solar power supply system with the existing flux tower.

In the experiment conducted in 2012, we deployed nine sink nodes in the LAINet area within a range of 4×4 km (4×4 1 km pixels with a spatial location corresponding to MODIS data). Each sink node was connected to three to nine measurement nodes using the Zigbee network. As a result, a total of 42 measurement nodes under the canopy and 3 above the canopy were established as in Fig. 1.

In Fig. 1, the sink nodes were powered by solar energy, and their antenna systems were fixed on 2.5 m supports to ensure that the signals were not sheltered by the canopy (which had a maximum height of 2.2 m). The three nodes above the canopy and their corresponding convergent antennas were deployed on the upper side of the same supports to ensure that the nodes above the canopy were not sheltered by other objects. The nodes under the canopy, which were powered by rechargeable lithium batteries, were positioned upward and perpendicularly to the corn ridges. Each node under the canopy was supported by a 20 cm brace to ensure that the node was not immersed in water during agricultural irrigation. All measurement and sink nodes were placed between 200 and 500 m apart. Data communication between the measurement and sink nodes was conducted directly or with a multi-hop mechanism. Therefore, the measured node data were easily transmitted by newly formed routes when the data were not transmitted directly to the sink node. The LAINet nodes are shown in Fig. 2.

In the course of the experiment, the sensors were set to operate from 09:00 to 18:00 h (the minimum value of the local solar elevation angle ranged from 26° to 32° and the maximum

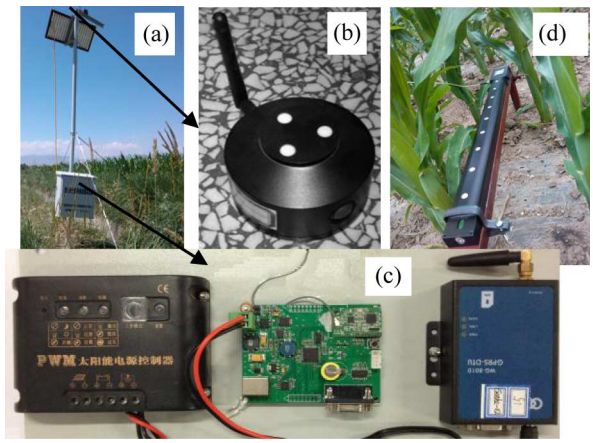

Fig. 2. LAINet nodes, including: (a) the solar power system, sink nodes, and nodes above the canopy, (b) the zoom of a node above the canopy, (c) the zoom of sink node (middle), the solar power control (left) and GPRS unit (right), and (d) a linear node with nine light sensors under the canopy.

value ranged from 67° to 81°). During this period, the sampling interval of the sensor was 15 min, with a sampling duration of 5 s. Therefore, during each 15-min sampling interval, the working duration was only 5 s. In addition, the sensor automatically shifted into sleep mode, which greatly reduced the instrument's energy consumption and extended its working duration. To evaluate the LAINet measurement results, we used the LAI-2000 to measure the vegetation LAI at locations in the experimental area that were near some of the nodes. To maintain the crop's stable growth around the LAINet site and to avoid human disturbance, the measured points of the LAI-2000

were placed at approximately 50–100 m from the LAINet node. The selection of the LAI-2000 sampling locations was based on the visible crop growth at the LAINet node to ensure that the growth status at the two types of measurement sites were alike. In the LAI-2000 measurement scheme, based on the instrument manual [28], an area of 5×5 m^2 was used to collect between 7 and 9 readings in a diagonal pattern. Next, the average value of the readings was used to calculate the LAI of the measured points. The measurement revisit period for the LAI-2000 was 5 days.

B. Data Processing

1) Multi-Angle Transmittance Calculations: WSN data were collected from the experimental area between June 25 and August 24, 2012. The data included the total solar radiation above the canopy and the transmitted radiation below the canopy. As mentioned above, three nodes above the canopy (which received the total solar radiation) were placed within the experimental area. We assumed that the solar radiation was uniformly distributed over an area of 4×4 km^2. Therefore, any of the three nodes could be integrated with the node data below to calculate the canopy transmittance.

The canopy transmittance was obtained by calculating the ratio of the radiation transmitted below the canopy to the total incident radiation above the canopy at different solar angles throughout the day. These calculations were performed as follows.

1) The solar elevation angle h was calculated based on the longitude, latitude, and local measurement time.
2) The start and end of the measurements above and below the canopy were read, and the overlapping time of the two nodes was calculated. Because the two types of nodes could work at different times, a uniform interpolation was applied to the observed sensor values within an overlapping time interval of 600 s. Therefore, the observations above and below the canopy were obtained at each time. These observations were denoted as E_0 and E_1, respectively.
3) The ratio of the observations below and above the canopy was calculated at each time to obtain the canopy transmittance at different solar elevation angles

$$T(h) = \frac{E_1}{E_0}. \tag{1}$$

2) LAI Calculations: The gap probability model for planted canopies was obtained based on the Poisson distribution [7], [29]

$$T(h) = e^{-\int_0^{\frac{\pi}{2}} A(\theta,h)\hat{g}(\theta)\mathrm{LAI}d\theta}. \tag{2}$$

In (2), θ represents the leaf inclination angle, h represents the solar elevation angle, $\hat{g}(\theta)$ is the distribution function of the leaf inclination angle, and $A(\theta, h)$ is a trigonometric function

$$A(\theta,h) = \begin{cases} \cos\ \theta, & \theta \le h \\ \cos\ \theta[1 + 2(\tan\ \theta_0 - \theta_0)/\pi], & h<\theta<\frac{\pi}{2}. \end{cases} \tag{3}$$

In (3), $\theta_0 = \mathrm{acos}(\tan h\ \cot\theta)$, we combined (2) and (3) and calculated the logarithms on both sides of (2) to obtain (4), as follows:

$$P(h) = -\ln(T(h)) = \int_0^{\frac{\pi}{2}} A(\theta,h)\hat{g}(\theta)\mathrm{LAI}\ d\theta. \tag{4}$$

Solving (4) required a continuous observation of $P(h)$; however, in practical observations, we could only obtain discrete transmittance values. Therefore, it was difficult to solve the integral equation (4) directly. However, (4) can also be written in a discrete form if

$$K(\theta, \boldsymbol{h}) = A(\theta, \boldsymbol{h})\hat{g}(\theta). \tag{5}$$

The leaf inclination angle was divided into $M + 1$ intervals with equal intervals within the range of $[0, \pi/2]$. The length of each interval was $\Delta\theta$. The average leaf inclination angle of the interval midpoint was θ_i, with $i \in [0, M]$. The LAI within the interval of each leaf inclination angle was L_i. Therefore, (4) can be written in a discrete form, as follows:

$$P(h_j) = \sum_{i=1}^{M} K(\theta_i, \boldsymbol{h_i})L_i, \quad j \in [1, N] \tag{6}$$

where N is the number of solar elevation angles.

When $M < N$, then L_i can be obtained by solving the first Fredholm equation. Next, the canopy LAI can be obtained using

$$\mathrm{LAI} = \sum_{i}^{M} L_i. \tag{7}$$

Before calculating the LAI, information regarding the leaf inclination angle was needed. According to Geol, the leaf inclination angle distribution patterns can be classified into six types [30]. Based on the previous results and field data, we assumed that the probability density function of the crop leaf inclination angle was vertical as

$$\hat{g}(\theta) = e^{0.583\theta - 1} \tag{8}$$

where the mathematical expectation of θ is 63.2°.

3) Calculation of the Regional Scale LAI from MODIS and ASTER Data: The MODIS LAI data were obtained within the same time range as the 2012 field experiment. The spatial resolution was 1 km and the time resolution was 8 days. The LAI data from multiple LAINet measurement nodes on the same day and within pixels that corresponded to the MODIS data were averaged to obtain the LAI data for each corresponding MODIS pixel.

Advanced Spaceborne Thermal Emission and Reflection Radiometer (ASTER) level 2 products with a resolution of 15 m, covering a time range from May 30 to September 19, 2012 were obtained from ASTER data's product distribution service website (http://gds.ersdac.jspacesystems.or.jp) and 6S model was used to transfer the ASTER data to the top of canopy reflectance [31]. All of the ASTER images were used to retrieve the high-resolution LAI, which will be used to scale up the ground LAINet observation to 1-km resolution satellite LAI when comparing it with the MODIS LAI. Because the MODIS LAI is estimated using 8 days of reflectance, the image data for the MODIS and ASTER sensors have a 1–2 day lag and the available images are listed in Table II. The satellite observation dates are also translated as a DOY (day of the year).

TABLE II
SATELLITE IMAGERY DATES FOR THE ASTER AND MODIS DATA

ASTER	Date	May-30	Jun-15	Jul-10	Aug-2	Aug-11	Aug-18	Aug-27	Sep-3	Sep-12	Sep-19
	DOY	151	167	192	215	224	231	240	247	256	263
MODIS	Date	Jun-01	Jun-17	Jul-11	Aug-4	Aug-12	Aug-20	Aug-28	Sep-5	Sep-13	Sep-21
	DOY	153	169	193	217	225	233	241	249	257	265

To relate the high spatial resolution radiometric data (here referred to as ASTER data) with the corresponding ground measurements (here referred to as LAINet), Baret *et al.* proposed two types of transfer functions that can either be derived from radiative transfer model inversion or can be purely empirical [25]. Here, the radiative transfer model inversion method is adopted to generate the ASTER LAI. The PROSAIL model, which is coupled with the SAIL [32] model and PROSPECT models [33], was inverted using a lookup table and a Bayesian network method as described in more detail in our other studies [34], [35]. In our method, the ground-measured LAINet LAI values are used to control the other free variables of the coupled radiative transfer model.

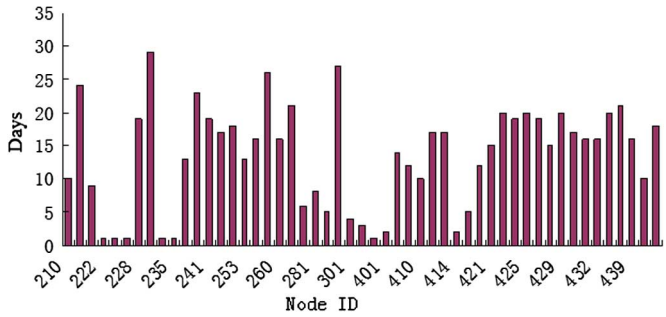

Fig. 3. Valid observation days for each node.

III. RESULTS AND DISCUSSION

A. Comparing the Measured Values of LAINet and the LAI-2000

Due to the unexpected battery and communication failures during the observations with LAINet, and due to cloudy and rainy days, not all measured LAINet values have corresponding LAI-2000 observations. Therefore, the number of comparable data pairs at each site is not the same. For every node deployed in the field from June 25 to August 24, the observation period lasts approximately up to 60 days, but due to the unexpected obstacles, the maximum valid observation days were approximately 30 and most of the nodes captured 2–3 days of LAI frequency (Fig. 3). As a result, to compare the measured results from the two different instruments, we used two adjacent instruments (within 100 m). The time gaps between the measurements were 1 or 2 days. The results of these comparisons between the measured LAINet and LAI-2000 values are presented in Fig. 4.

As shown in Fig. 4, the coefficients of determination (R^2) from comparing the results were between 0.28 and 0.97, with an average R^2 of 0.42. These results indicated that the differences between the data measured with the two different instruments varied by site. The highest relevant difference appeared at the EC06 site. At this site, the data were collected from June 25 ($\mathrm{DOY} = 177$) to August 11 ($\mathrm{DOY} = 224$) with the LAINet values measured between 1.6 and 3.4. The lowest relevant difference was observed at the EC14 site, where the greatest difference between the two instruments was observed when the LAI values were lower than 1.5 or greater than 3.0.

In Fig. 4, when the LAI was lower than 3.5, the LAI-2000 estimates were greater than the LAINet estimates. Conversely, when the LAI values were higher than 3.5, the observed LAI-2000 values were lower than the LAINet values. Unfortunately, the LAI destructive value for corn crops was not obtained in this study. Although the current measurements did not clarify in which the instrument was more accurate, many researchers have indicated that the LAI-2000 estimates are lower than the true LAI values. This finding was most notable when the LAI was relatively large, in which case the observed LAI-2000 values were much lower than their true values. For example, by comparing the canopy LAI of broad-leaf and coniferous forests, Martens *et al.* [36] determined that the Li–Cor light quantum meter estimates (which used the direct light method as our method in this study) were greater than the LAI-2000 estimates. Compared with the direct measurement method, the Li–Cor light quantum meter method was the most accurate. Other researchers have reported similar results. For example, Mason *et al.* discovered that the ratio of direct measurement values to the LAI-2000 values was approximately 1.5 [10], [12]. We had similar findings. When the LAI was relatively large (higher than 3.5), the average ratio of the observed LAINet value (with the direct light principle) to the LAI-2000 value was approximately 1.3. This result indicated that the measured LAINet value was potentially closer to the true LAI value of the crop. However, this conclusion needs to be validated with true ground measurements in the further work.

B. Time Series Analysis

1) Time Series at the Single Node: The models used to describe the law of dynamic changes of LAI can be categorized as having linear and nonlinear methods [37], [38]. As this paper does not focus on the LAI simulation model, we simply choose a quadratic polynomial simulation model to describe the dynamic changes of the LAI. As shown in Fig. 5, the dynamic growth characteristics for corn crops in the Heihe River experimental area were present in the observed LAINet data at all of the sites, with the exception of the EC13 (S02-4), where no continuous observations were made. A common feature was identified from the dynamic curve fitting of the LAI at sites EC15 (S01-3), EC14 (S04-1), and EC08 (S06-2). The time series observation results in the Heihe River

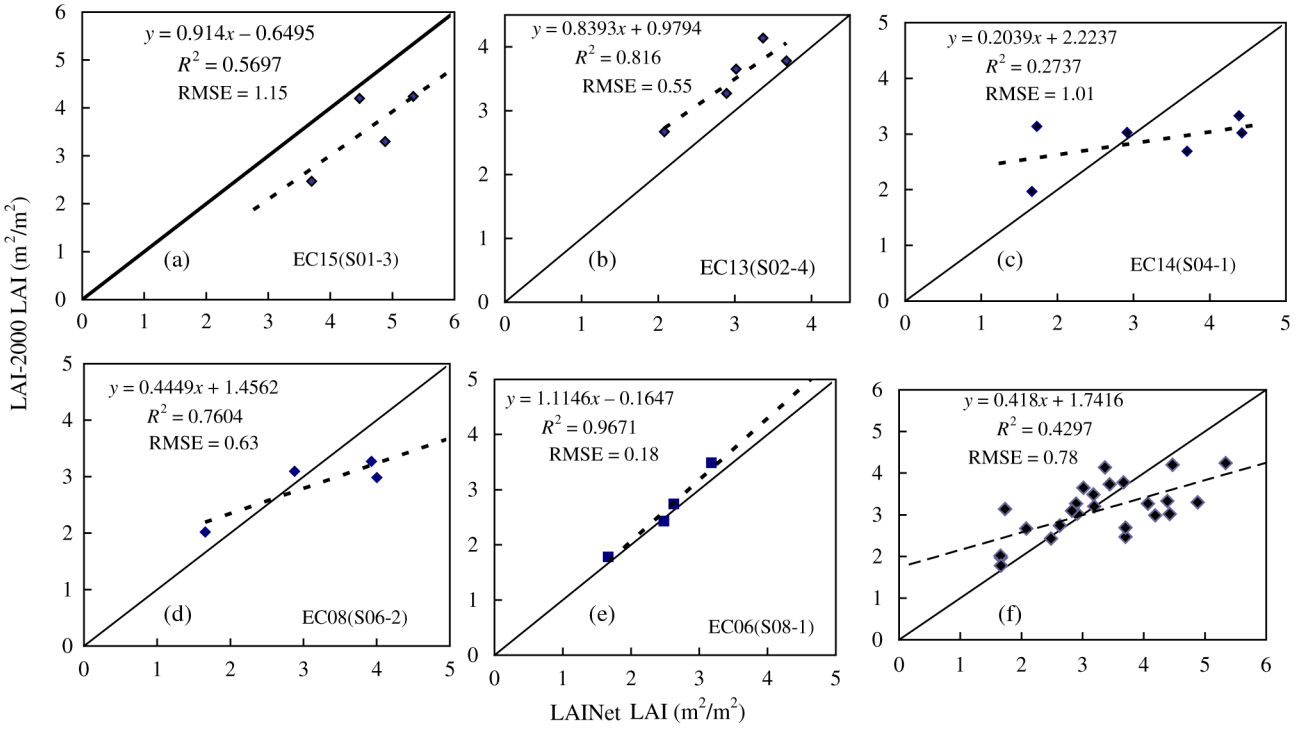

Fig. 4. Scatter plots of the measured LAI values for the LAINet and LAI-2000 observations.

area indicated that the corn crop LAI reached a maximum value between DOY 207 and DOY 210, before it began to decrease.

However, at the EC06 (S08-1) site, the fitting results in the time series were worse than the results for the other three nodes mentioned above. At this site, the observed LAI value fluctuated significantly, especially near DOY 232. However, when comparing the LAINet observations with the LAI-2000 values (on the days when comparable data were available for both instruments), a high relative coefficient was obtained, as shown in Fig. 4(e). Although the abnormal fluctuations at the EC06 (S08-1) site could not be explained, it may be inferred that the growth condition of the crops around this site was potentially disturbed by external influence, such as crop management (irrigation, fertilization, etc.).

Although most of the observed LAINet values potentially indicated good dynamic crop growth characteristics over time, there are still some daily LAI values that varied only slightly on each observation day [Fig. 5(e)]. These variations on consecutive days potentially resulted from the different weather conditions on different observation days. Due to daily changes in the weather, the proportion of the scattered light in the sky varied at different observation times. The Beer–Lambert law applies only when describing the attenuation of direct canopy sunlight. The presence of scattered light creates measurement errors when monitoring the transmittance of the direct light. These errors were then brought into the LAI estimation process.

Fig. 5 also shows that after the canopy nears the complete closure, most of the measured LAINet values are higher than the values of the LAI-2000, which may be due to the fact that the LAI-2000 measures the transmittance of canopy diffusion light and is more easily saturated at high LAI values when compared with the instruments that use the transmittance of beam light to estimate the LAI. When the corn crop leaves reach a maximum size, the measurement results of the LAI-2000 will underestimate the true values. In the published literature [36], the authors compared the measurement results of the LAI-2000 and other instruments that use the sun's direct transmitted PAR to estimate the canopy LAI. They found that among the different results, the LAI-2000 usually produced the lowest LAI. Our observation results are essentially consistent with the existing research.

2) Time Aggregation of the LAINet LAI: To investigate the reliability of the observations at a single node and to describe the dynamic characteristics of the crops in the time series, we selected three nodes with relatively complete observed LAINet data. The LAI is a structure parameter reflecting the vegetation growth. The growth of the crop leaves requires time for the accumulation of material energy. Although there is not a definite value that properly describes the timing of the leaf growth, the model simulation results [37], actual measurements [38], and the repeat-visit period of remote sensing satellites [39] suggested that most people accepted a time frequency of 3–8 days as an adequate to describe the dynamic process of leaves. Therefore, in this section, we selected an aggregating window of 5 days to process the filed data. Then, we used the measured LAI data, with a time resolution of 5 days, to fit the time-series distribution from DOY 177 (from June 25 to 29, 2012) to DOY 232 (from August 19 to 23, 2012) (Fig. 6). The solid lines in the plots are the quadratic curve fitting results.

As shown in Fig. 6, the measured values at a single node that were averaged by a time window of 5 days represented the dynamic variations in the corn crop LAI in the experiment area. The R^2 of the quadratic curve fitting results were 0.76, 0.92, and 0.92, respectively, which indicated that the observed values in the time series were parabolic in shape. These plots clearly

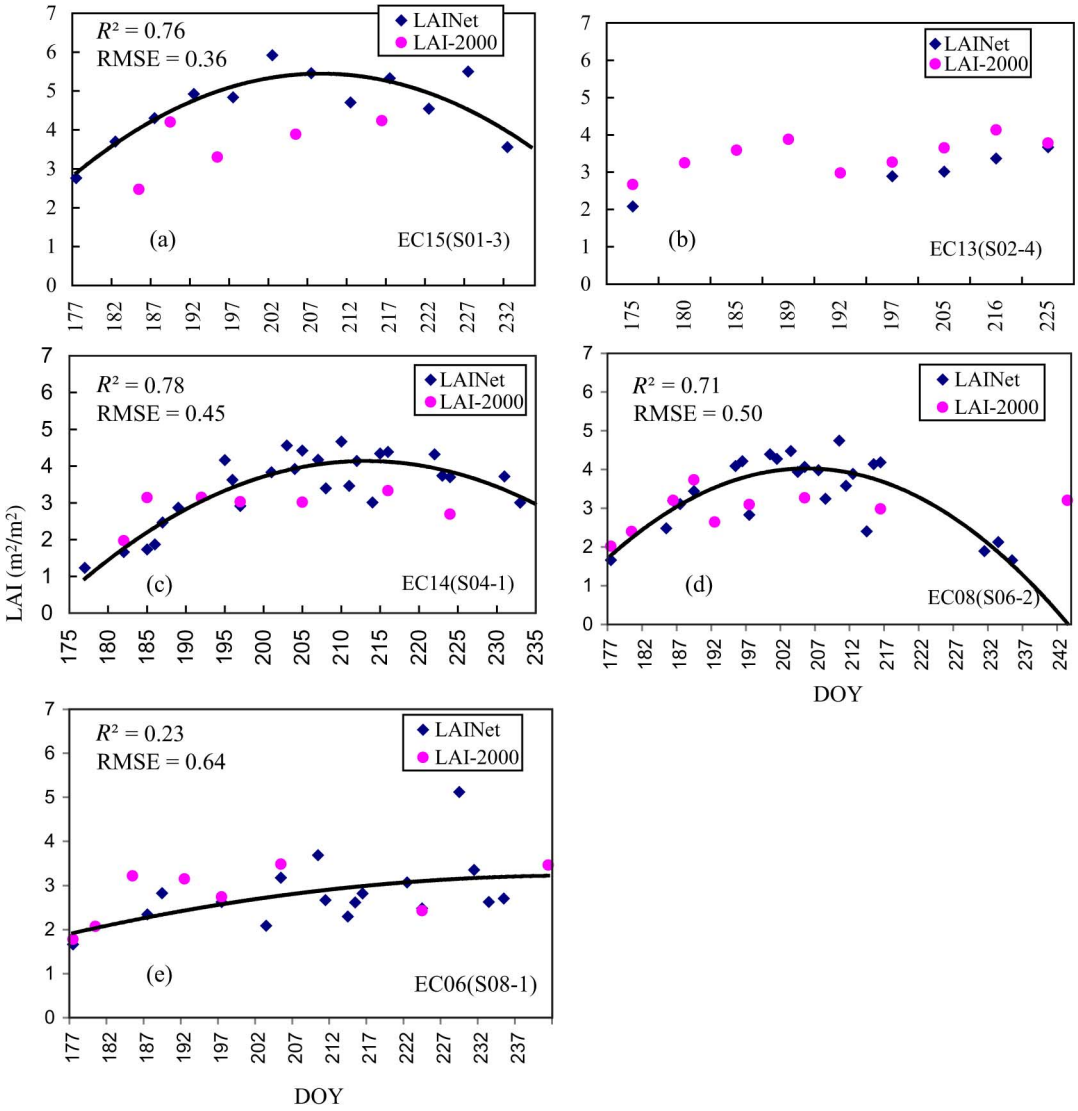

Fig. 5. Comparison between the measured LAINet and LAI-2000 data in the time series. Plots (a)–(e) correspond to plots (a)–(e) in Fig. 4, respectively. The solid lines in plot (a) and (c)–(e) were generated using quadratic curve fitting.

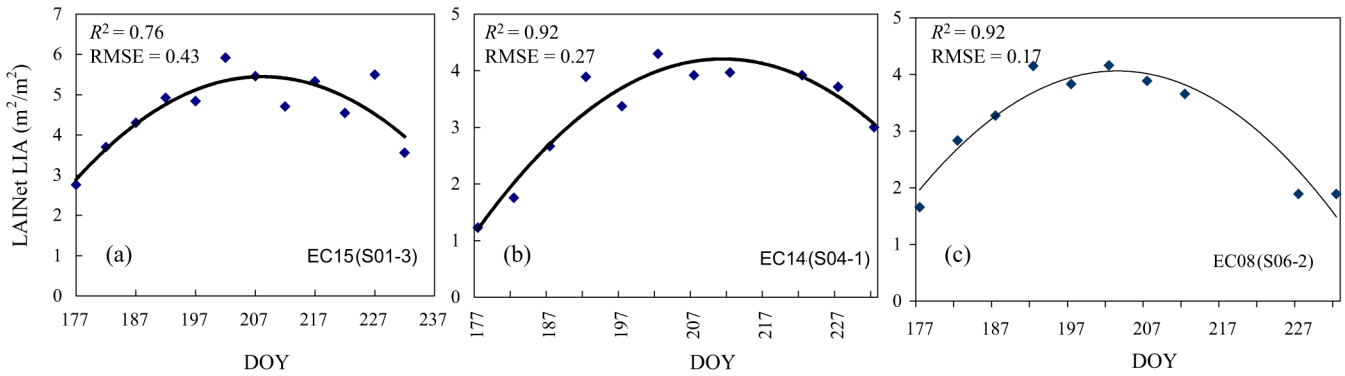

Fig. 6. Time series plots of the measured values at a single node averaged over 5 days.

show the increasing and decreasing LAI values between DOY 207 and DOY 212. In addition, the maximum LAIs were 5.9, 4.3, and 4.2, respectively.

The time aggregation results suggested that an aggregation time of 5 days might be enough to describe the crop growth trajectory. The vegetation LAI has different observed time resolutions at different growth stages. During the rapid growth or decline stages, the LAI values vary widely. Generally, an observation resolution of 3 days is appropriate. When the growth is near or reaches its maximum, a stable period generally occurs.

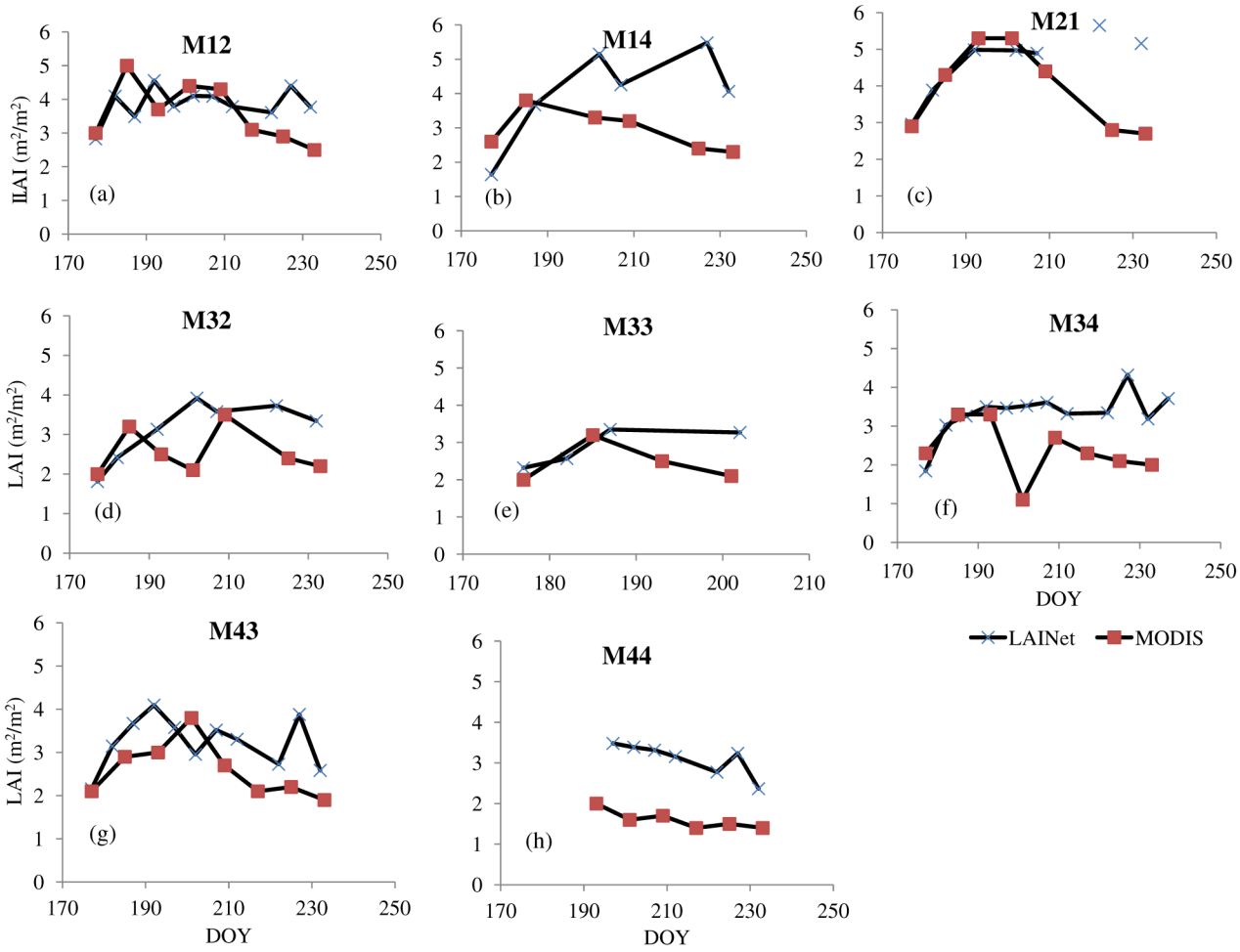

Fig. 7. Comparison of the time series between MODIS LAI products and the LAINet LAI.

During this stable period, the time resolution of the LAI observations can be reduced to between 5 and 10 days. Here, the proposed LAINet used a stationary observation method, which allowed for the availability of daily data, and made it possible to obtain the average data for different time windows.

C. Comparison With MODIS LAI

In the area corresponding to each MODIS pixel, we deployed multiple LAINet nodes on the ground. The comparison with MODIS LAI was conducted in two ways: by directly comparing the ground value with MODIS LAI and scaling up the ground-measured LAI to a 1-km resolution using high-resolution imagery as a bridge.

First, we directly averaged the multi-node LAI values in the corresponding pixels and compared them with the LAI values of the corresponding MODIS pixels in the time series (Fig. 7). Although ground-measured LAI values are recommended for scaling up using a high-resolution image to relate the ground measurements of the LAI with those derived from the MODIS data [11], here, we simply present a direct comparison results from the perspective of the overall numerical data value and the data's time trends between the ground LAINet measurement and the MODIS LAI. The uncertainty of the mismatch of the viewing footprint and the data scale is discussed below.

In general, the LAI values of the LAINet exhibited identical or similar trends to those of the MODIS LAI values in the time series. For example, in Fig. 7, the M12, M32, M43, and M44 trends were the same, whereas the M21 and M33 trends were more consistent at the growth stage than during the decline stage. Regarding the MODIS LAI time variations, the dates on which the MODIS LAI reached its maximum growth stage varied between DOY 195 and DOY 210. The maximum values of some pixels were obtained earlier than the LAINet observation dates. Most of the LAINet LAI values were greater than the MODIS LAI values. This result might be explained by the different observation scales and the spatial heterogeneity of the objects.

LAI trends of change over time show estimated differences between LAINet and MODIS and are greater in the descending phase of the LAI, which may result from the principles of the two estimation methods. The MODIS LAI is retrieved by inverting the canopy spectral reflectance. After the leaf size reaches its maximum and begins to decrease, even though the leaf area may not obviously change, some leaves may turn yellow, which causes the spectral reflectance of the leaves to decrease in the green band and to increase in the red band. Therefore, inverting the satellite data at this time according to the radiation transfer equation will underestimate the actual LAI; however, LAINet estimates the LAI by measuring the gap probability under the canopy at this point, so if the sizes and the number of leaves do

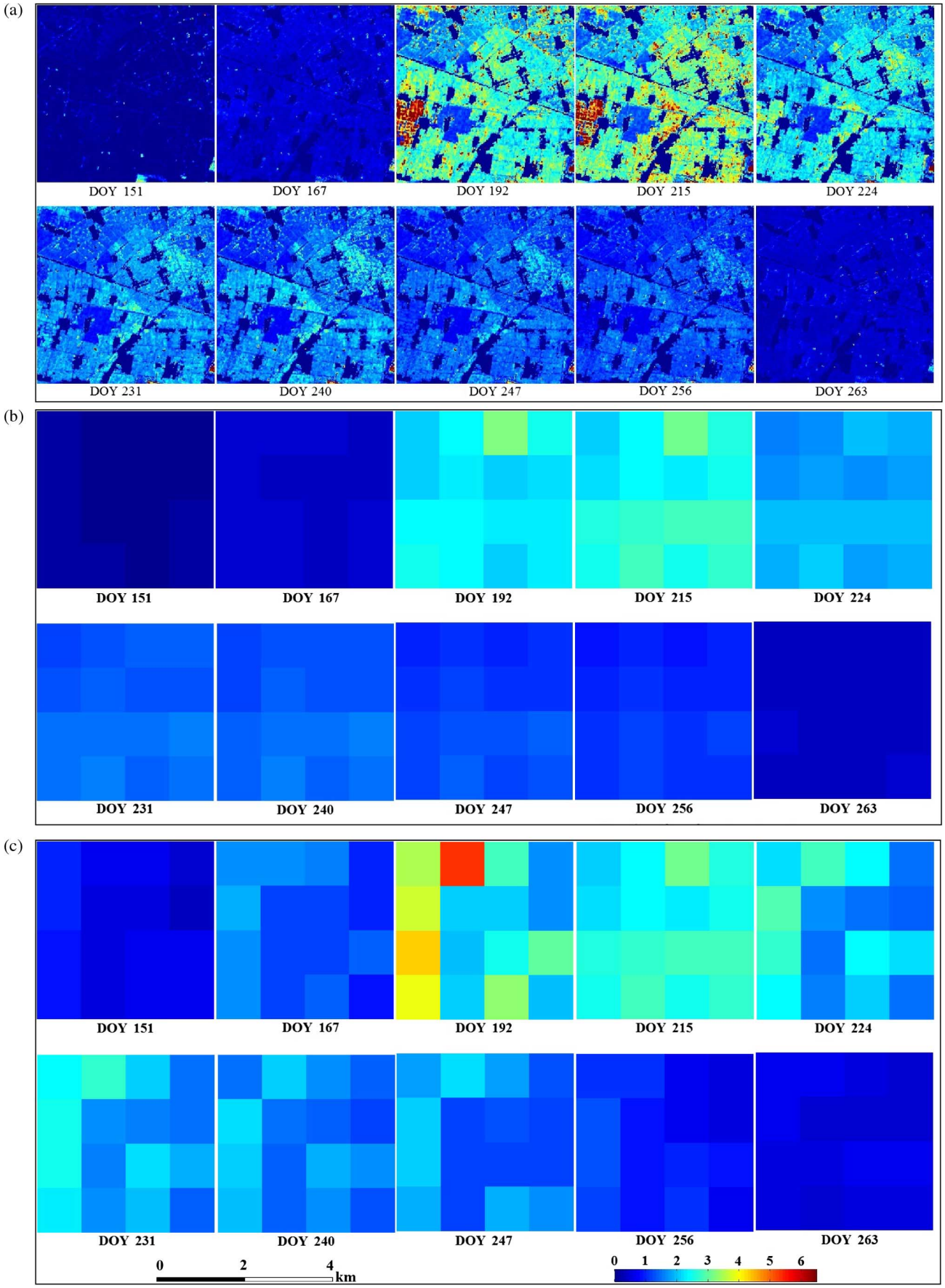

Fig. 8. Mapping the LAI in the experimental area for: (a) a 15-m resolution LAI map from ASTER data, (b) a scaled-up 1-km resolution LAI, and (c) a MODIS 1-km resolution LAI.

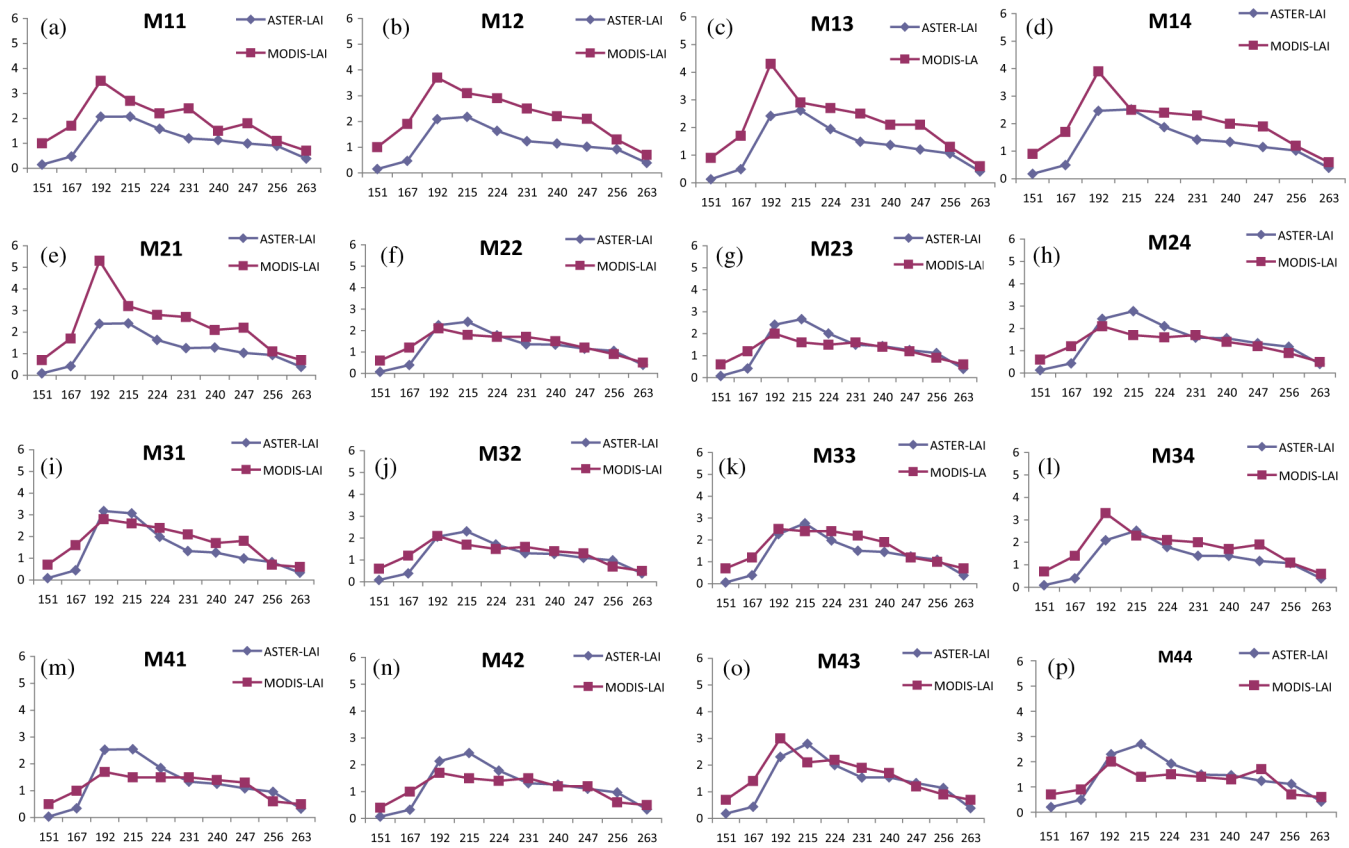

Fig. 9. Comparison of the MODIS LAI and aggregated 1-km resolution ASTER LAI in a time series.

not change significantly, the LAI estimated by LAINet cannot exhibit sharp variations and even the MODIS LAI begins to descend. Another reason may be that LAINet measures the total contribution of the leaves and stem, whereas the satellite measures the leaf reflectance on the top of canopy. Therefore, inverting the LAI using satellite data is more responsive to changes in the canopy leaves than LAINet, and the LAINet LAI values are greater than the estimated values of the MODIS data.

Secondly, we compared the MODIS LAI with a scaled-up LAI that was retrieved from the ASTER data after spatial aggregation (Fig. 8). Because the resolution rate between the MODIS and ASTER LAI was a nonintegral zoom factor, the retrieved 15-m resolution ASTER LAI [Fig. 8(a)] was aggregated into a 1-km resolution [Fig. 8(b)] by a bilinear interpolation method that considers the closest 2×2 neighborhood of the ASTER pixel values surrounding the target MODIS pixel [40]. The aggregation procedure was accomplished by MATLAB Image Processing Toolbox (The Math Works, Inc., Natick, MA, USA). The MODIS LAI products are also shown in Fig. 8(c).

We compared the two types of LAIs based on the time series of each pixel. As shown in Fig. 9, the LAIs of two satellite products had the same trends for the time series of most pixels. Especially for the 11 pixels (f–p) from M22 to M44 pixel, in all of these 11 pixels, the two types of LAIs are very close to both in value and in trend. For the other five pixels (a–e), although the trends of the LAI are very similar, the MODIS LAI is greater than the inversion result of the ASTER data. The deviation is partly explained by the singular large values of the MODIS LAI data. For example, in the three pixels (c–e), the MODIS LAI suddenly increased abnormally on DOY 192. Another primary reason may be explained by the complexity of land cover types. In the five pixels (a–e), many residential areas were scattered. When the ASTER inversion was performed on these pixels, they were masked as nonvegetation areas. The inversion of the LAI by MODIS did not distinguish the land cover types of the subpixels in the MODIS pixel.

As some vegetables, fruit trees, and scattered woodlands are distributed in these regions, the LAI value inverted by MODIS was higher than the LAI value of the ASTER data in these regions. This deviation in the inversion result may be caused by the complexity of land cover types and was not obvious in other pixels due to the decrease in the proportion of residential areas. When comparing the inversion results of the two satellites for all of the time series in the whole region, we also found that the inversion results of the ASTER data were slightly lower than the MODIS LAI on the whole (Fig. 10) with an $R^2 = 0.5029$ and $\mathrm{RMSE} = 0.7035$.

The 2012 experiment sought to determine if better spatial representation could be obtained by carefully identifying the position and number of sensor nodes when deploying the MODIS pixels to cover more land types, considering the heterogeneity of the vegetation cover. Adequate spatial sampling will be conducted in future studies in the research area with the goal of obtaining a statistically significant canopy gap probability. In traditional studies, the spatial distribution of the canopy gap probability, or gap size, is measured manually. In the method

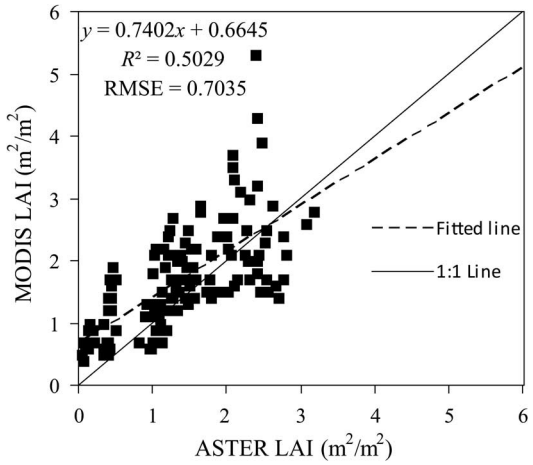

Fig. 10. Scatter plot between ASTER LAI and MODIS LAI in 4×4 pixels from DOY 151 to DOY 263.

proposed in this paper, this is accomplished by deploying a high number of nodes under the canopy.

IV. Conclusion

We developed an automatic system for measuring the vegetation LAI with WSN technology. Continuous time series LAI observations were conducted on corn crops in the Heihe River basin. A comparative analysis was conducted between different ground measurement instruments and data obtained from MODIS.

The WSN technology is particularly useful for data collection and remote transmission because it can improve the automotive data acquisition and reduce human disturbance. The LAI measurement method proposed in this paper can be used to measure the vegetation canopy structure parameters over long periods at a regional scale. Therefore, the method has the potential to support ground validation for surface parameters obtained by the remote sensing.

We found that the measured LAINet values may be more accurate than the LAI-2000 values, particularly when the LAI is greater than 3.5. The determination coefficient (R^2) between the observed LAINet and LAI-2000 values ranged from 0.28 to 0.97. In general, when the LAI was greater than 3.5, the observed LAI-2000 values changed dynamically over a small range, which did not fully reflect the dynamic LAI changes. Regarding the average value of the corresponding observed data, the observed LAINet value was greater than the LAI-2000 value (with a ratio of approximately 1.3). The comparison results between the measured and true LAI-2000 values reported in the literature showed that when the LAI is > 3.0, the LAI-2000 underestimates the true LAI values. The ratio of the true-to-measured values is approximately 1.5. This is consistent with the experimental results presented in this paper.

As discussed above, one advantage of LAINet is its ability to provide continuous observations of the vegetation growth process. The LAI time series observation results indicated that the observed LAINet data properly described the growth process for corn crops in the Heihe River watershed. The data that the LAI reached its maximum matched the satellite observation data in 2012.

We calculated the observed LAINet value and compared it with the satellite data from two aspects, which included a direct method and a scaled-up method. When directly comparing the ground LAINet LAI with a 1-km resolution MODIS LAI, we found that the LAINet data, which were greater than the MODIS data, were similar to the MODIS LAI results regarding changes over time. When the aggregated ASTER LAI derived from a radiative transfer model inversion into a 1-km resolution, the ASTER LAI in most pixels behaved similar to the MODIS LAI values and the time series trends. However, we also observed that there was a slight discrepancy in the few of the pixels. The inconsistencies might be explained by the different footprints of the observed objects, the differences between the land-cover classes, and the observation time resolution. In the future, we plan to deploy the LAINet observation nodes more carefully to obtain actual surface cover conditions.

Light diffusion significantly affected the observed LAINet values. Currently, many instruments or observation methods are used to obtain the proportion of light diffusion. In the future, we plan to determine the proportions of scattered light at different times to increase the precision of the LAI inversion when LAINet is used for observations.

Some other factors that can improve the robustness of LAINet may be considered for further validation. For example, the real-time data storing strategy may prevent the data from being lost in the case where a GPRS network does not work properly. The low energy consumption allows the instruments to function for extended periods. However, due to the operational capability of the power supply system (lithium batteries), the energy consumption is strongly affected by the temperature. The expected working hours were not fully achieved in the arid environment of the research area, which might have resulted from high temperatures in the corn canopy when the ambient air temperatures were high. We plan to improve the instrument performance and minimize the manual maintenance in the future studies. With these improvements, the instruments may function continuously for longer periods.

References

[1] J. M. Chen and T. A. Black, "Measuring leaf area index of plant canopies with branch architecture," *Agri. Forest Meteorol.*, vol. 57, no. 1, pp. 1–12, Dec. 1991.

[2] W. B. Cohen, T. K. Maiersperger, Z. Yang, S. T. Gower, D. P. Turner, W. D. Ritts, M. Berterretche, and S. W. Running, "Comparisons of land cover and LAI estimates derived from ETM+ and MODIS for four sites in North America: A quality assessment of 2000/2001 provisional MODIS products," *Remote Sens. Environ.*, vol. 88, no. 3, pp. 233–255, 2003.

[3] S. Garrigues, N. V. Shabanov, K. Swanson, J. T. Morisette, F. Baret, and R. B. Myneni, "Intercomparison and sensitivity analysis of leaf area index retrievals from LAI-2000, AccuPAR, and digital hemispherical photography over croplands," *Agri. Forest Meteorol.*, vol. 148, no. 8–9, pp. 1193–1209, Jul. 2008.

[4] N. J. J. Bréda, "Ground-based measurements of leaf area index: A review of methods, instruments and current controversies," *J. Exp. Bot.*, vol. 54, no. 392, pp. 2403–2417, 2003.

[5] D. Arias, J. Calvo-Alvarado, and A. Dohrenbusch, "Calibration of LAI-2000 to estimate leaf area index (LAI) and assessment of its relationship with stand productivity in six native and introduced tree species in Costa Rica," *Forest Ecol. Manag.*, vol. 247, no. 1/3, pp. 185–193, 2007.

[6] K. R. Whitford, I. J. Colquhoun, A. R. G. Lang, and B. M. Harper, "Measuring leaf area index in a sparse eucalypt forest: A comparison of estimates from direct measurement, hemispherical photography, sunlight

transmittance and allometric regression," *Agri. Forest Meteorol.*, vol. 74, no. 3–4, pp. 237–249, May 1995.
[7] A. R. G. Lang and X. Yueqin, "Estimation of leaf area index from transmission of direct sunlight in discontinuous canopies," *Agri. Forest Meteorol.*, vol. 37, no. 3, pp. 229–243, Aug. 1986.
[8] Y. Ryu, J. Verfaillie, C. Macfarlane, H. Kobayashi, O. Sonnentag, R. Vargas, S. Ma, and D. D. Baldocchi, "Continuous observation of tree leaf area index at ecosystem scale using upward-pointing digital cameras," *Remote Sens. Environ.*, vol. 126, pp. 116–125, Nov. 2012.
[9] X. Li, G. Cheng, S. Liu, Q. Xiao, M. Ma, R. Jin, T. Che, Q. Liu, W. Wang, Y. Q, J. Wen, H. Li, G. Zhu, J. Guo, Y. Ran, S. Wang, Z. Zhu, J. Zhou, X. Hu, and Z. Xu, "Heihe watershed allied telemetry experimental research (HiWATER): Scientific objectives and experimental design," *Bull. Amer. Meteorol. Soc.*, vol. 94, no. 8, pp. 1145–1160, Aug. 2013.
[10] E. G. Mason, M. Diepstraten, G. L. Pinjuv, and J.-P. Lasserre, "Comparison of direct and indirect leaf area index measurements of *Pinus radiata* D. Don," *Agri. Forest Meteorol.*, vol. 166–167, pp. 113–119, 2012.
[11] J. T. Morisette, F. Baret, J. L. Privette, R. B. Myneni, J. E. Nickeson, S. Garrigues, N. V. Shabanov, M. Weiss, R. A. Fernandes, S. G. Leblanc, M. Kalacska, G. A. Sanchez-Azofeifa, M. Chubey, B. Rivard, P. Stenberg, M. Rautiainen, P. Voipio, T. Manninen, A. N. Pilant, T. E. Lewis, J. S. Iiames, R. Colombo, M. Meroni, L. Busetto, W. B. Cohen, D. P. Turner, E. D. Warner, G. W. Petersen, G. Seufert, and R. Cook, "Validation of global moderate-resolution LAI products: A framework proposed within the CEOS land product validation subgroup," *IEEE Trans. Geosci. Remote Sens.*, vol. 44, no. 7, pp. 1804–1817, Jul. 2006.
[12] A. R. G. Lang, "Simplified estimate of leaf area index from transmittance of the sun's beam," *Agri. Forest Meteorol.*, vol. 41, no. 3–4, pp. 179–186, Dec. 1987.
[13] A. Suri, S. S. Iyengar, and E. Cho, "Ecoinformatics using wireless sensor networks: An overview," *Ecol. Informat.*, vol. 1, no. 3, pp. 287–293, Nov. 2006.
[14] P. W. Rundel, E. A. Graham, M. F. Allen, J. C. Fisher, and T. C. Harmon, "Environmental sensor networks in ecological research," *New Phytol.*, vol. 182, pp. 589–607, 2009.
[15] R. Morais, M. A. Fernandes, S. G. Matos, C. Serôdio, P. J. S. G. Ferreira, and M. J. C. S. Reis, "A ZigBee multi-powered wireless acquisition device for remote sensing applications in precision viticulture," *Comput. Electron. Agri.*, vol. 62, pp. 94–106, 2008.
[16] D. Liping, K. Moe, and T. L. van Zyl, "Earth observation sensor web: An overview," *IEEE J. Sel. Top. Appl. Earth Obs. Remote Sens.*, vol. 3, no. 4, pp. 415–417, Dec. 2010.
[17] P. M. Teillet, "Sensor webs: A geostrategic technology for integrated earth sensing," *IEEE J. Sel. Top. Appl. Earth Obs. Remote Sens.*, vol. 3, no. 4, pp. 473–480, Dec. 2010.
[18] M. Moghaddam, D. Entekhabi, Y. Goykhman, L. Ke, L. Mingyan, A. Mahajan, A. Nayyar, D. Shuman, and D. Teneketzis, "A wireless soil moisture smart sensor web using physics-based optimal control: Concept and initial demonstrations," *IEEE J. Sel. Top. Appl. Earth Obs. Remote Sens.*, vol. 3, no. 4, pp. 522–535, Dec. 2010.
[19] A. Zerger, R. A. Viscarra Rossel, D. L. Swain, T. Wark, R. N. Handcock, V. A. J. Doerr, G. J. Bishop-Hurley, E. D. Doerr, P. G. Gibbons, and C. Lobsey, "Environmental sensor networks for vegetation, animal and soil sciences," *Int. J. Appl. Earth Obs. Geoinf.*, vol. 12, pp. 303–316, 2010.
[20] J. K. Hart and K. Martinez, "Environmental sensor networks: A revolution in the earth system science?," *Earth Sci. Rev.*, vol. 78, pp. 177–191, 2006.
[21] J. A. López Riquelme, F. Soto, J. Suardíaz, P. Sánchez, A. Iborra, and J. A. Vera, "Wireless sensor networks for precision horticulture in Southern Spain," *Comput. Electron. Agri.*, vol. 68, pp. 25–35, 2009.
[22] P. Loden, Q. Han, L. Porta, T. Illangasekare, and A. P. Jayasumana, "A wireless sensor system for validation of real-time automatic calibration of groundwater transport models," *J. Syst. Softw.*, vol. 82, pp. 1859–1868, 2009.
[23] Y. Yuan, L. Shanshan, W. Kui, J. Weijia, and P. Yuxing, "FOCUS: A cost-effective approach for large-scale crop monitoring with sensor networks," in *Proc. IEEE 6th Int. Conf. Mobile Adhoc and Sensor Systems (MASS '09), Macau SAR, China,,* 2009, pp. 544–553.
[24] Y. Qu, J. Wang, J. Dong, and F. Jiang, "Design and experiment of crop structural parameters automatic measurement system," *Trans. CSAE*, vol. 28, pp. 160–165, 2012 (in Chinese with English abstract).
[25] F. Baret, M. Weiss, M. Leroy, D. Allard, S. Garrigues, H. Bohbot, R. Bosseno, C. D. Bella, M. Espana, V. Gond, J.-P. Guinot, D. Guyon, C. Lelong, E. Mougin, T. Nilson, and R. Vintilla, VALERI: A network of sites and a methodology for the validation of land satellite products [Online]. Available: http://w3.avignon.inra.fr/valeri/documents/, 2003.
[26] F. Baret, J. T. Morissette, R. A. Fernandes, J. L. Champeaux, R. B. Myneni, J. Chen, S. Plummer, M. Weiss, C. Bacour, S. Garrigues, and J. E. Nickeson, "Evaluation of the representativeness of networks of sites for the global validation and intercomparison of land biophysical products: Proposition of the CEOS-BELMANIP," *IEEE Trans. Geosci. Remote Sens.*, vol. 44, no. 7, pp. 1794–1803, Jul. 2006.
[27] S. Garrigues, D. Allard, F. Baret, and M. Weiss, "Influence of landscape spatial heterogeneity on the nonlinear estimation of leaf area index from moderate spatial resolution remote sensing data," *Remote Sens. Environ.*, vol. 105, pp. 286–298, 2006.
[28] Li-Cor, Inc., LAI-2000 plant canopy analyzer, *Instruction Manual.* Lincoln, NE, USA: Li-Cor, Inc.,1991.
[29] T. Nilson, "Inversion of gap frequency data in forest stands," *Agri. Forest Meteorol.*, vol. 98–99, pp. 437–448, 1999.
[30] N. S. Goel, "Models of vegetation canopy reflectance and their use in estimation of biophysical parameters from reflectance data," *Remote Sens. Rev.*, vol. 4, pp. 1–212, 1988.
[31] E. F. Vermote, D. Tanre, J. L. Deuze, M. Herman, and J. J. Morcette, "Second simulation of the satellite signal in the solar spectrum, 6S: An overview," *IEEE Trans. Geosci. Remote Sens.*, vol. 35, no. 3, pp. 675–686, May 1997.
[32] W. Verhoef, "Light scattering by leaf layers with application to canopy reflectance modeling: The SAIL model," *Remote Sens. Environ.*, vol. 16, pp. 125–141, 1984.
[33] S. Jacquemoud and F. Baret, "PROSPECT: A model of leaf optical properties," *Remote Sens. Environ.*, vol. 34, pp. 75–91, 1990.
[34] Y. Qu, Y. Zhang, and J. Wang, "A dynamic Bayesian network data fusion algorithm for estimating leaf area index using time-series data from in situ measurement to remote sensing observations," *Int. J. Remote Sens.*, vol. 33, pp. 1106–1125, 2012.
[35] Y. Qu, Y. Zhang, and H. Xue, "Retrieval of 30-m-resolution leaf area index from China HJ-1 CCD data and MODIS products through a dynamic Bayesian network," *IEEE J. Sel. Top. Appl. Earth Obs. Remote Sens.*, vol. PP, no. 99, pp. 1–7, Jun. 2013.
[36] S. N. Martens, S. L. Ustin, and R. A. Rousseau, "Estimation of tree canopy leaf area index by gap fraction analysis," *Forest Ecol. Manag.*, vol. 61, pp. 91–108, 1993.
[37] C. Damgaard, "Modelling individual plant growth at a variable mean density or at a specific spatial setting," *Biol. Model.*, vol. 327, pp. 255–260, 2004.
[38] U. Karadavut, Ç. Palta, K. Kökten, and A. Bako lu, "Comparative study on some nonlinear growth models for describing leaf growth of maize," *Int. J. Agri. Biol.*, vol. 12, pp. 227–230, 2010.
[39] Q. Wang, J. Tenhunen, N. Q. Dinh, M. Reichstein, D. Otieno, A. Granier, and K. Pilegarrd, "Evaluation of seasonal variation of MODIS derived leaf area index at two European deciduous broadleaf forest sites," *Remote Sens. Environ.*, vol. 96, pp. 475–484, 2005.
[40] E. Kirkland, "Bilinear interpolation," *Advanced Computing in Electron Microscopy*, New York, NY, USA: Springer, 2010, pp. 261–263.

Yonghua Qu received the M.Sc. degree in geology from China University of Mining Technology, Jiangsu, China, in 2000, and the Ph.D. degree in remote sensing from the Beijing Normal University, Beijing, China, in 2005.

From 2007 to 2012, he held a position as Assistant Professor in the School of Geography at Beijing Normal University, Beijing, China. Since March 2012, he has been working as a Project Leader in remote sensing inversion using dynamic Bayesian network which is supported by National Natural Science Foundation of China, China.

Yeqing Zhu received the B.S. degree in geographical information system from Yanshan University, Hebei, China, in 2011. She is currently pursuing the Master degree in cartography and geographical information system at Beijing Normal University, Beijing, China.

Her research interests focus on the leaf biochemical content retrieval using radiative transfer model and heavy metal-polluted vegetation hyper-spectral data.

Wenchao Han received the B.S. degree in geography from Northwest Normal University, Lanzhou, China, in 2012, and he is currently pursuing the Master degree in cartography and geographical information system at Beijing Normal University, Beijing, China.

His research interests focus on the algorithms for retrieving LAI using dynamic Bayesian network.

Jindi Wang received the B.S. degree from the Beijing University of Posts and Telecommunications, Beijing, China, in 1982.

She is currently a Professor with the State Key Laboratory of Remote Sensing Science, Beijing Normal University/Chinese Academy of Sciences, and the School of Geography, Beijing Normal University, Beijing, China. Her primary research interests focus on land surface BRDF modeling, land surface parameters retrieval from various remotely sensed data, especially from time series observations and by combined dynamic model.

Mingguo Ma received the B.Sc. degree in 1998 from Lanzhou University, Gansu, China, and the Ph.D. degree in 2003 from Cold and Arid Regions Environmental and Engineering Research Institute (CAREERI), Chinese Academy of Sciences (CAS), Beijing, China.

From November 2003 to March 2009, he held a position as Assistant Professor at the Laboratory of Remote Sensing and Geospatial Science, CAREERI, CAS, Beijing, China. Since April 2009, he is a Professor at the Laboratory of Remote Sensing and Geospatial Science, CAREERI, CAS, Beijing, China. His main research interests have been in monitoring and simulating the vegetation cover change, retrieval and validation of terrestrial biophysical parameters in northwest China.